PERGAMON

International Journal of Solids and Structures 36 (1999) 465–487

INTERNATIONAL JOURNAL OF SOLIDS and STRUCTURES

A theoretical study of the coupling effects in piezoelectric ceramics

Xiaoping Ruan[a], Stephen C. Danforth[b], Ahmad Safari[b], Tsu-Wei Chou[a,*]

[a]*Center for Composite Materials and Department of Mechanical Engineering, University of Delaware, Newark, DE 19716, U.S.A.*

[b]*Department of Ceramic and Material Engineering and Center for Ceramic Research, Rutgers, The State University of New Jersey, Piscataway, NJ 08855, U.S.A.*

Received 16 October 1997; in revised form 13 January 1998

Abstract

The objective of this study is to delineate electro-mechanical coupling in piezoceramic materials. The model system investigated is a two-dimensional linear piezoceramic strip polarized in the thickness direction, and it is subjected to local symmetric pressures on the upper and lower edges, traction-free boundary conditions on both end surfaces, and voltages on portions of the upper and lower edges. Under a simplifying assumption of the gradient of the electric potential, closed form solutions of the elastic field have been obtained.

It is noticed that instead of the nine constants (including the elastic compliance constants, s_{ij}, the piezoelectric constants, d_{ij}, and the dielectric permittivity constants, ε_{ij}), the elastic and piezoelectric characteristics of the material can be represented by three parameters, β_1, β_2 and β_3. β_1 consists of elastic compliance constants only. β_2 and β_3 signify the piezoelectric effect. Furthermore, higher values of β_2 imply a more pronounced piezoelectric effect on the elastic field. The identification of these parameters greatly facilitates the study of coupling effects in piezoelectric ceramics. © 1998 Elsevier Science Ltd. All rights reserved.

1. Introduction

Piezoelectricity is the characteristic of certain materials to develop an electric charge when a mechanical stress is applied (direct effect), or to develop a deformation when a voltage is applied (converse effect). In piezoelectric ceramics, when an electrical field is applied parallel to the polarization direction, an expansion in the same direction and shrinkage in the transverse direction occur. When an electrical field is applied perpendicular to the polarization direction, shear defor-

* Author to whom correspondence should be addressed. Fax: 3028313619. E-mail: chou@me.udel.edu

0020–7683/99/$ - see front matter © 1998 Elsevier Science Ltd. All rights reserved.
PII: S0020–7683(98)00026–2

mation occurs (Tiersten, 1969). Significant advances have been made in recent years in the technologies of piezoelectric materials and their applications, for example, in intelligent structures (Newnham, 1997), various types of metal-ceramic composite actuators (Newnham *et al.*, 1992; Dogan and Newnham, 1994), and multi-phase piezoelectric composite transducers (Zhang *et al.*, 1995).

Although the theory of linear piezoelectricity is well developed, analytical solutions of the coupled electric and elastic fields are often limited to problems with fairly simple geometry and boundary conditions. The analyses and models in the literature pertaining to electro-mechanical devices are mostly based upon the finite element method (FEM) (see, for instance, Tzou and Tseng, 1990; Kagawa *et al.*, 1996). Although FEM is very useful in the analysis of piezoelectric devices, it does not effectively delineate the interrelationship among the various piezoelectric and elastic constants, namely, their coupling effects. Overall, FEM is not highly desirable for parametric studies. The purpose of this paper is to pursue an analytical approach for demonstrating the effects of the elastic and piezoelectric characteristics (including the elastic compliance constants, s_{ij}, the piezoelectric constants, d_{ij}, and the dielectric permittivity constants, ε_{ij}) on the electric and stress fields of a 2-D piezoceramic strip. Although the boundary value problem examined here is relatively simple, the conclusions derived from this exercise are of general applicability.

In this paper, a closed form solution for a 2-D linear piezoceramic strip under stress and electric boundary conditions is developed using the Airy stress function and the electric potential function. The piezoceramic strip polarized in the thickness direction is subjected to local symmetric pressures on the upper and lower edges, traction-free boundary conditions on both end surfaces, as well as voltages on portions of the upper and lower edges. First, it is assumed that the gradient of electric potential in the strip length-wise direction is much smaller than that in the thickness direction. Thus, the governing equations in terms of the Airy stress function and electric potential can be uncoupled. Then, the solutions to the governing equations are sought in the form of Fourier series. Finally, the results of electric and stress fields obtained from the analytical approach are compared with those obtained from FEM analysis, and the effects of material constants on the electric and stress fields are evaluated in terms of three non-dimensional parameters.

2. Theory

2.1. *Constitutive equations and governing equations of piezoelectricity*

The constitutive equations of piezoelectricity can be stated in the following general form:

$$\{\mathbf{S}\} = [\mathbf{s}]\{\boldsymbol{\sigma}\} + [\mathbf{d}]\{E\} \tag{1}$$

$$\{\mathbf{D}\} = [\mathbf{d}]^T\{\boldsymbol{\sigma}\} + [\boldsymbol{\varepsilon}]\{E\} \tag{2}$$

where $\{\boldsymbol{\sigma}\}$ = stress tensor in contracted notation, $\{\mathbf{S}\}$ = strain tensor in contracted notation, $\{E\}$ = electric field vector, $\{\mathbf{D}\}$ = electric displacement vector, $[\mathbf{s}]$ = elastic compliance matrix, $[\mathbf{d}]$ = piezoelectric constant matrix, and $[\boldsymbol{\varepsilon}]$ = dielectric permittivity matrix. The equation of motion and the charge equation of electrostatics are, respectively

$$\sigma_{ij,i} + f_j = \rho\ddot{u}_j \tag{3}$$

$$D_{i,i} = 0 \tag{4}$$

where σ_{ij} = stress tensor, f_j = body force, u_j = displacement, D_i = electric displacement, and ρ = density.

Consider a 2-D problem in the $x_1 - x_3$ plane. If the x_3-axis is taken as the polarization direction, the constitutive equation for a piezoelectric ceramic can be written as:

$$\begin{Bmatrix} S_1 \\ S_3 \\ S_5 \end{Bmatrix} = \begin{bmatrix} s_{11} & s_{13} & 0 \\ s_{13} & s_{33} & 0 \\ 0 & 0 & s_{55} \end{bmatrix} \begin{Bmatrix} \sigma_1 \\ \sigma_3 \\ \sigma_5 \end{Bmatrix} + \begin{bmatrix} 0 & d_{31} \\ 0 & d_{33} \\ d_{15} & 0 \end{bmatrix} \begin{Bmatrix} E_1 \\ E_3 \end{Bmatrix} \tag{5}$$

$$\begin{Bmatrix} D_1 \\ D_3 \end{Bmatrix} = \begin{bmatrix} 0 & 0 & d_{15} \\ d_{31} & d_{33} & 0 \end{bmatrix} \begin{Bmatrix} \sigma_1 \\ \sigma_3 \\ \sigma_5 \end{Bmatrix} + \begin{bmatrix} \varepsilon_{11} & 0 \\ 0 & \varepsilon_{33} \end{bmatrix} \begin{Bmatrix} E_1 \\ E_3 \end{Bmatrix} \tag{6}$$

The equation of equilibrium (with zero body force) and the compatibility equation are, respectively,

$$\frac{\partial \sigma_1}{\partial x_1} + \frac{\partial \sigma_5}{\partial x_3} = 0$$

$$\frac{\partial \sigma_5}{\partial x_1} + \frac{\partial \sigma_3}{\partial x_3} = 0 \tag{7}$$

$$\frac{\partial^2 S_1}{\partial x_3^2} + \frac{\partial^2 S_3}{\partial x_1^2} = \frac{\partial^2 S_5}{\partial x_1 \, \partial x_3} \tag{8}$$

2.2. *Governing equations in terms of Airy stress function and electric potential*

Substituting the constitutive equation [eqn (5)] into the compatibility equation [eqn (8)], we get

$$\frac{\partial^2}{\partial x_3^2}[s_{11}\sigma_1 + s_{13}\sigma_3 + d_{31}E_3] + \frac{\partial^2}{\partial x_1^2}[s_{13}\sigma_1 + s_{33}\sigma_3 + d_{33}E_3] = \frac{\partial^2}{\partial x_1 x_3}[s_{55}\sigma_5 + d_{15}E_1] \tag{9}$$

which is expressed in terms of the stress and electric fields. Substituting the constitutive equation [eqn (6)] into the charge equation [eqn (4)] yields

$$\frac{\partial}{\partial x_1}[d_{15}\sigma_5 + \varepsilon_{11}E_1] + \frac{\partial}{\partial x_3}[d_{31}\sigma_1 + d_{33}\sigma_3 + \varepsilon_{33}E_3] = 0 \tag{10}$$

which is also given in terms of the stress and electrical fields.

The Airy stress function $f(x_1, x_3)$ is defined such that

$$\sigma_1 = \frac{\partial^2 f}{\partial x_3^2}, \quad \sigma_3 = \frac{\partial^2 f}{\partial x_1^2}, \quad \sigma_5 = -\frac{\partial^2 f}{\partial x_1 x_3} \tag{11}$$

The equations of equilibrium [eqn (7)] are then identically satisfied. An electric potential, φ, is introduced, and the electric field can be expressed as

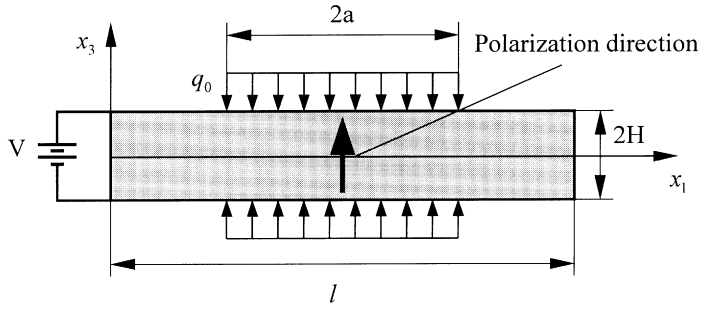

Fig. 1. A piezoceramic strip with boundary conditions.

$$E_1 = -\frac{\partial \varphi}{\partial x_1}, \quad E_3 = -\frac{\partial \varphi}{\partial x_3} \tag{12}$$

Finally, substituting the Airy stress function and electric potential into eqns (9) and (10), we obtain the following governing equations:

$$s_{11}\frac{\partial^4 f}{\partial x_3^4} + (2s_{13} + s_{55})\frac{\partial^4 f}{\partial x_1^2 x_3^2} + s_{33}\frac{\partial^4 f}{\partial x_3^4} = d_{31}\frac{\partial^3 \varphi}{\partial x_3^3} + (d_{33} - d_{15})\frac{\partial^3 \varphi}{\partial x_1^2 x_3} \tag{13}$$

$$\varepsilon_{11}\frac{\partial^2 \varphi}{\partial x_1^2} + \varepsilon_{33}\frac{\partial^2 \varphi}{\partial x_3^2} = d_{31}\frac{\partial^3 f}{\partial x_3^3} + (d_{33} - d_{15})\frac{\partial^3 f}{\partial x_1^2 x_3} \tag{14}$$

which involves all nine independent elastic, piezoelectric and dielectric constants.

2.3. *Governing equations for a piezoelectric strip*

Consider a piezoelectric strip that occupies the region $0 \leqslant x_1 \leqslant l$, $-H \leqslant x_3 \leqslant H$ as shown in Fig. 1. Here H is the half thickness of the strip, and l is the length of the strip. The strip is polarized in the x_3-direction. Symmetric loads are applied on the upper and lower edges of the strip, and voltages are also added on the upper and lower edges. A traction-free boundary condition exists on both ends of the strip.

We consider the case that the constant voltages are applied on the upper and lower edges, and it is reasonable to assume that the x_3 component of the electric field, E_3, is much greater than the x_1 component, E_1. Thus, $(\partial\varphi/\partial x_3) \gg (\partial\varphi/\partial x_1)$. If it is further assumed that $\partial^2\varphi/\partial x_3^2$ is much greater than $\partial^2\varphi/\partial^2 x_1$, we can neglect the last term of eqn (13), and the first term of eqn (14). Then, eqns (13) and (14) yield

$$s_{11}\frac{\partial^4 f}{\partial x_3^4} + (2s_{13} + s_{55})\frac{\partial^4 f}{\partial x_1^2 x_3^2} + s_{33}\frac{\partial^4 f}{\partial x_3^4} = d_{31}\frac{\partial^3 \varphi}{\partial x_3^3} \tag{15}$$

$$\varepsilon_{33}\frac{\partial^2 \varphi}{\partial x_3^2} = d_{31}\frac{\partial^3 f}{\partial x_3^3} + (d_{33} - d_{15})\frac{\partial^3 f}{\partial x_1^2 x_3} \tag{16}$$

Taking the partial derivative of x_3 to eqn (16) and then substituting it into eqn (15), the governing equation in terms of the stress function only is obtained:

$$s_{11}\frac{\partial^4 f}{\partial x_3^4}+\left[(2s_{13}+s_{55})-\frac{d_{31}}{\varepsilon_{33}}(d_{33}-d_{15})\right]\frac{\partial^4 f}{\partial x_1^2 x_3^2}+\left(s_{33}-\frac{d_{31}^2}{\varepsilon_{33}}\right)\frac{\partial^4 f}{\partial x_3^4}=0 \tag{17}$$

2.4. *Non-dimensionalization*

In order to reduce the number of independent constants, the governing partial differential equations [eqns (16) and (17)] are first non-dimensionalized. The dimensionless co-ordinates ξ and η are defined as

$$\xi=\left(\frac{s_{11}}{s_{33}}\right)^{1/4}\frac{x_1}{H},\quad \eta=\frac{x_3}{H}$$

Also, by defining the following non-dimensional constants

$$\beta_1=\left(\frac{1}{s_{11}s_{33}}\right)^{1/2}(2s_{13}+s_{44})$$

$$\beta_2=\frac{d_{31}^2}{\varepsilon_{33}s_{11}}$$

$$\beta_3=\left(\frac{1}{s_{11}s_{33}}\right)^{1/2}\frac{d_{31}}{\varepsilon_{33}}(d_{33}-d_{15}) \tag{18}$$

and the dimensional constant

$$\kappa=\frac{d_{31}}{s_{11}}$$

the governing partial differential eqns (17) and (16) become, respectively,

$$\frac{\partial^4 f}{\partial\xi^4}+(\beta_1-\beta_3)\frac{\partial^4 f}{\partial\xi^2\eta^2}+(1-\beta_2)\frac{\partial^4 f}{\partial\eta^4}=0 \tag{19}$$

$$\frac{\partial^2\varphi}{\partial\eta^2}=\frac{1}{H}\frac{\beta_3}{\kappa}\frac{\partial^3 f}{\partial\xi^2\eta}+\frac{1}{H}\frac{\beta_2}{\kappa}\frac{\partial^3 f}{\partial\eta^3} \tag{20}$$

where H is the half thickness of the strip. The governing equations in the above form involve three non-dimensional constants and one dimensional constant rather than nine material constants. Furthermore, eqn (19) pertains to the Airy stress function only, and it does not involve the electric potential function.

2.5. *Fourier series solution*

We seek solution of eqn (19) in the form of Fourier series

$$f(\xi,\eta)=\sum_{n=1}^{\infty}\sin\alpha_n\xi F_n(\eta) \tag{21}$$

where $\alpha_n=n\pi/L$, and $L=(s_{11}/s_{33})^{1/4}(l/H)$, which represents the transformed strip length. This form is so chosen that the normal stress, σ_1, at both ends of the strip vanishes. Substituting eqn (21) into eqn (19) gives a fourth-order ordinary differential equation in $F_n(\eta)$:

$$\gamma_2 F''''_n(\eta)-\gamma_1\alpha_n^2F''_n(\eta)+\alpha_n^4F_n(\eta)=0\quad(n=1,2\ldots\infty) \tag{22}$$

Here, we seek solutions to eqn (22) in the form

$$F_n(\eta)=e^{\lambda_n\eta} \tag{23}$$

Substituting eqn (23) into eqn (22), the following characteristic equation is obtained:

$$\gamma_2\lambda_n^4-\gamma_1\alpha_n^2\lambda_n^2+\alpha_n^4=0 \tag{24}$$

where $\gamma_1=\beta_1-\beta_3$, $\gamma_2=1-\beta_2$. The roots of eqn (24) are

$$\lambda_n=\pm\frac{\alpha_n}{\sqrt{2\gamma_2}}\sqrt{\gamma_1\pm\sqrt{\gamma_1^2-4\gamma_2}} \tag{25}$$

Considering the case $\gamma_1^2-4\gamma_2<0$, which is valid for all the piezoceramics studied here, the four roots of λ_n can be denoted as

$$\lambda_{n1},\lambda_{n2}=p_n\pm iq_n,\quad \lambda_{n3},\lambda_{n4}=-p_n\pm iq_n$$

where $i=\sqrt{-1}$.

The general solution of eqn (22) is expressed as

$$F_n(\eta)=e^{p_n\eta}(C_{n1}\cos q_n\eta+C_{n2}\sin q_n\eta)+e^{-p_n\eta}(C_{n3}\cos q_n\eta-C_{n4}\sin q_n\eta) \tag{26}$$

The constants of integration C_{n1}, C_{n2}, C_{n3} and C_{n4} can be determined by the boundary conditions on the upper and lower edges. For the case of the symmetric loading in the present problem, it can be shown that $C_{n3}=C_{n1}$, and $C_{n4}=C_{n2}$. Therefore, we have

$$F_n(\eta)=(e^{p_n\eta}+e^{-p_n\eta})C_{n1}\cos q_n\eta+(e^{p_n\eta}-e^{-p_n\eta})C_{n2}\sin q_n\eta \tag{27}$$

The stress components are then given by

$$\sigma_1=\frac{1}{H^2}\sum_{n=1}^{\infty}\sin\alpha_n\xi F''_n(\eta)$$

$$\sigma_3=-\frac{1}{H^2}\left(\frac{s_{11}}{s_{33}}\right)^{1/2}\sum_{n=1}^{\infty}\alpha_n^2\sin\alpha_n\xi F_n(\eta)$$

$$\sigma_5 = -\frac{1}{H^2}\left(\frac{s_{11}}{s_{33}}\right)^{1/4}\sum_{n=1}^{\infty}\alpha_n\cos\alpha_n\xi F_n'(\eta) \tag{28}$$

where $F_n'(\eta)$ and $F_n''(\eta)$ are given in the Appendix.

We also seek $\varphi(\xi,\eta)$ in the form of

$$\varphi(\xi,\eta) = \sum_{n=1}^{\infty}\sin\alpha_n\xi G_n(\eta) \tag{29}$$

Substituting eqn (29) into eqn (20) yields

$$G_n''(\eta) = -\alpha_n^2\frac{\beta_3}{\kappa H}F_n'(\eta) + \frac{\beta_2}{\kappa H}F'''_n(\eta) \tag{30}$$

Integrating eqn (30) twice with respect to η, we obtain

$$G_n(\eta) = -\alpha_n^2\frac{\beta_3}{\kappa H}I_n(\eta) + \frac{\beta_2}{\kappa H}F_n'(\eta) + D_{n1}\eta + D_{n2} \tag{31}$$

where

$$I_n(\eta) = \int F_n(\eta)\,\mathrm{d}\eta$$

and it is given in the Appendix. D_{n1} and D_{n2} are the constants of integration.

Finally, from eqns (31) and (12), the electric fields are obtained

$$E_1 = -\frac{1}{H}\left(\frac{s_{11}}{s_{33}}\right)^{1/4}\sum_{n=1}^{\infty}\alpha_n G_n(\eta)\cos\alpha_n\xi$$

$$E_3 = -\frac{1}{H}\sum_{n=1}^{\infty}\alpha_n G_n'(\eta)\sin\alpha_n\xi \tag{32}$$

The strain components and electric displacement components can be determined by substituting eqns (28) and (32) into eqns (5) and (6).

2.6. *Boundary conditions*

The mechanical and electric boundary conditions examined in this paper (Fig. 1) are stated as follows:

on the upper edge ($x_3 = H$)

$$q_u(x_1) = \begin{cases} q_0 & \dfrac{l}{2} - a \leqslant x_1 \leqslant \dfrac{l}{2} + a \\ 0 & \text{elsewhere} \end{cases} \tag{33}$$

$$V_u(x_1) = \begin{cases} V_1 & \frac{l}{2} - b \leqslant x_1 \leqslant \frac{l}{2} + b \\ 0 & \text{elsewhere} \end{cases} \tag{34}$$

and on the lower edge ($x_3 = -H$)

$$q_l(x_1) = q_u(x_1) \tag{35}$$

$$V_l(x_1) = \begin{cases} V_0 & \frac{l}{2} - b \leqslant x_1 \leqslant \frac{l}{2} + b \\ 0 & \text{elsewhere} \end{cases} \tag{36}$$

where $q_u(x_1)$, $q_l(x_1)$ are applied pressure, and $V_u(x_1)$, $V_l(x_1)$ are applied voltage. a and b are the half lengths over which pressure and voltage are applied, respectively.

Rewriting the boundary conditions [eqns (33)–(36)] in terms of the non-dimensional variables, we have:

on the upper edge

$$q_u(\xi) = \begin{cases} q_0 & \frac{L}{2} - A \leqslant \xi \leqslant \frac{L}{2} + A \\ 0 & \text{elsewhere} \end{cases} \tag{37}$$

$$V_u(\xi) = \begin{cases} V_1 & \frac{L}{2} - B \leqslant \xi \leqslant \frac{L}{2} - B \\ 0 & \text{elsewhere} \end{cases} \tag{38}$$

and on the lower edge

$$q_l(\xi) = q_u(\xi) \tag{39}$$

$$V_l(\xi) = \begin{cases} V_0 & \frac{L}{2} - B \leqslant \xi \leqslant \frac{L}{2} - B \\ 0 & \text{elsewhere} \end{cases} \tag{40}$$

where L, A and B are the transformed quantities given by

$$L = \left(\frac{s_{11}}{s_{33}}\right)^{1/4} \frac{l}{H}, \quad A = \left(\frac{s_{11}}{s_{33}}\right)^{1/4} \frac{a}{H}, \quad \text{and} \quad B = \left(\frac{s_{11}}{s_{33}}\right)^{1/4} \frac{b}{H}$$

Also, $q_u(\xi)$, $q_l(\xi)$, $V_u(\xi)$ and $V_l(\xi)$ can be expanded in Fouriers series as follows:

$$q_u(\xi) = \sum_{n=1}^{\infty} b_n \sin \alpha_n \xi$$

$$q_l(\xi) = q_u(\xi)$$

$$V_u(\xi) = \sum_{n=1}^{\infty} d_n \sin \alpha_n \xi$$

$$V_l(\xi) = \sum_{n=1}^{\infty} e_n \sin \alpha_n \xi \tag{41}$$

The coefficients b_n, d_n and e_n can be determined as

$$b_n = \frac{4q_0}{n\pi} \sin\left(\frac{n\pi}{2}\right) \sin \alpha_n A$$

$$d_n = \frac{4V_1}{n\pi} \sin\left(\frac{n\pi}{2}\right) \sin \alpha_n B$$

$$e_n = \frac{4V_0}{n\pi} \sin\left(\frac{n\pi}{2}\right) \sin \alpha_n B \tag{42}$$

For the case of the symmetric loading in the present problem, the boundary conditions of eqns (33)–(36) are expressed below in terms of the stress components and electric potential:

$$\begin{aligned} &\sigma_3 = -q_u(x_1) \quad x_3 = +H \\ &\sigma_5 = 0 \quad x_3 = +H \\ &\varphi = V_u(x_1) \quad x_3 = +H \\ &\varphi = V_l(x_1) \quad x_3 = -H \end{aligned} \tag{43}$$

Rewriting the above boundary conditions in terms of $F_n(\eta)$ and $G_n(\eta)$ using the non-dimensional variables, results in

$$\begin{aligned} &F_n(\eta) = \frac{b_n}{\rho_n} \quad \eta = +1 \\ &F_n'(\eta) = 0 \quad \eta = +1 \quad (n = 1, 2, \ldots, N) \\ &G_n(\eta) = d_n \quad \eta = 1 \\ &G_n(\eta) = e_n \quad \eta = -1 \end{aligned} \tag{44}$$

where

$$\rho_n = \frac{1}{H^2} \left(\frac{s_{11}}{s_{33}}\right)^{1/2} \alpha_n^2$$

Equation (44) stands for $4N$ equations, and all the $4N$ constants can be determined. The expressions of C_{n1}, C_{n2}, D_{n1} and D_{n2} are given in the Appendix.

Finally, we re-examine all the boundary conditions of the piezoelectric strip. On the upper and lower edges, the stress and electric boundary conditions are identically satisfied. The traction-free

boundary conditions at both ends of the strip require that $\sigma_1 = 0$, $\sigma_5 = 0$, and $D_1 = 0$. From eqn (28), it can be seen that

$$\sigma_1 = 0, \quad \int_{-H}^{+H} \sigma_5 \, dx_3 = 0 \quad \text{at } x_1 = 0, \quad \text{and} \quad x_1 = l$$

Also, by assuming that $E_1 = 0$ for the present problem, eqn (6) gives $D_1 = d_{15}\sigma_5$, and it can be readily shown that

$$\int_{-H}^{H} D_1 \, dx_3 = 0 \quad \text{at } x_1 = 0, \quad \text{and} \quad x_1 = l$$

Thus, the boundary conditions at both end surfaces of the strip are approximately satisfied.

3. Numerical example and results

The numerical example performed for the piezoceramic strip focuses on PZT-5H, whose material properties are listed in Table 1. The geometric parameters are $l = 10$ mm, and $H = 1$ mm. The mechanical and electric loadings are $q_0 = 20$ N/mm^2 ($2.5 \leqslant x_1 \leqslant 7.5$ mm) and $V_u = 1000$ V ($0 \leqslant x_1 \leqslant 10$ mm) and $V_l = 0$ ($0 \leqslant x_1 \leqslant 10$ mm).

Table 1
Elastic, piezoelectric and dielectric constants of some selected piezoceramics

	PZT-5H[a]	PZT-5[b]	PZT-4[c]	Ceramic −B[a]	VIBRIT 200[d]	VIBRIT 525[d]
Elastic components (10^{-12} m^2/N)						
s_{11}	16.5	16.4	12.4	8.6	11.1	15.7
s_{12}	−4.78	−5.74	−3.98	−2.6	−4.4	−5.9
s_{13}	−8.45	−7.22	−5.52	−2.7		
s_{33}	20.7	18.8	16.1	9.1	12.1	19.3
s_{44}	43.5	47.5	39.1	22.2	27.0	46.0
Piezoelectric constant (10^{-12} C/N)						
d_{31}	−274	−172	−135	−58	−80	−190
d_{33}	593	374	300	149	170	420
d_{15}	741	584	525	242	220	625
Relative permittivity ($\varepsilon_0 = 8.85 \times 10^{-12}$ F/m)						
$\varepsilon_{11}/\varepsilon_0$	1700	1730	1470	1000	900	2000
$\varepsilon_{33}/\varepsilon_0$	1470	1700	1300	910	1030	2000

[a] Data Sheet (1990); [b] Rogacheva (1994); [c] Park and Sun (1995); [d] Zelenka (1986).

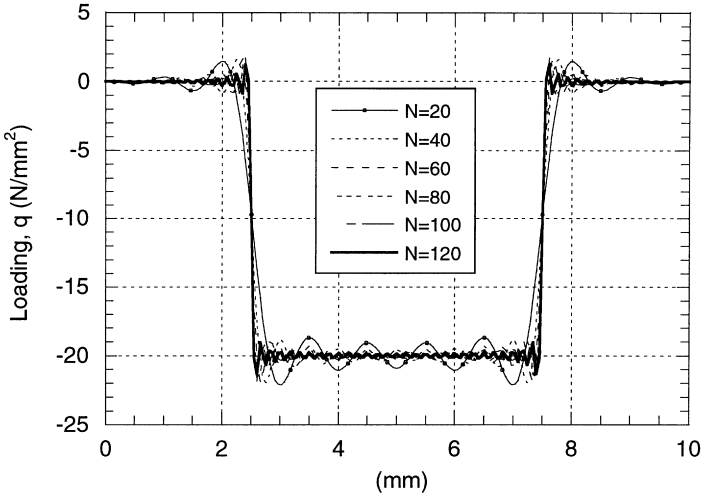

Fig. 2. Partial summations of Fourier series.

For all the Fourier expressions discussed above, the first 120 terms are used to represent the infinite series, which are adequate for the purpose of convergence. Figure 2 plots the partial summations of Fourier series representing distributed pressure on the surface of the piezoceramic strip in order to examine their convergence. It can be seen that when the number of terms (N) used in the series summation is 120, the discrepancy is less than 2% except for the overshoot at the discontinuity. For the purpose of assessing the capability of the present closed form solution, a parallel numerical analysis is also conducted using the commercially available FEM code ABAQUS for linear piezoelectric materials. We use 384 8-node serendipity elements for one-half of the piezoceramic strip.

Figures 3–5 show the distribution of the stress components, σ_1, σ_3, and σ_5 in one quarter of the piezoceramic strip using a closed form solution (a), and an FEM approach (b). The distributions of electric potential in the piezoelectric strip obtained by the analytical model and the FEM approach are shown, respectively, in Fig. 6(a) and (b).

It can be seen from Figs 3–6 that the result obtained from the closed form solution are in very good agreement with those from the FEM approach. A comparison of the results obtained from these two approaches shows that the largest difference of the stress components, σ_1, σ_3 and σ_5 occurs around $x_1 = 7.5$ mm, the edge of the distributed load. There is a change of sign of σ_1 and σ_3, around $x_1 = 7.5$ mm, and σ_5 reaches its maximum at this location. Along the symmetric axis ($x_3 = 0$), the change of stress components, σ_1, σ_3 and σ_5, becomes gradual compared to the stress components along the edges. The variation of electric potential, φ, is almost linear along the x_3 axis.

The electric potential on the upper edge near the end of the strip obtained from the closed form solution is not very satisfactory, and there is about 11% overshoot compared with the prescribed boundary values. Again, this is attributed to the Gibbs phenomenon, associated with the Fourier series representation of any function with a jump discontinuity (Greenberg, 1988).

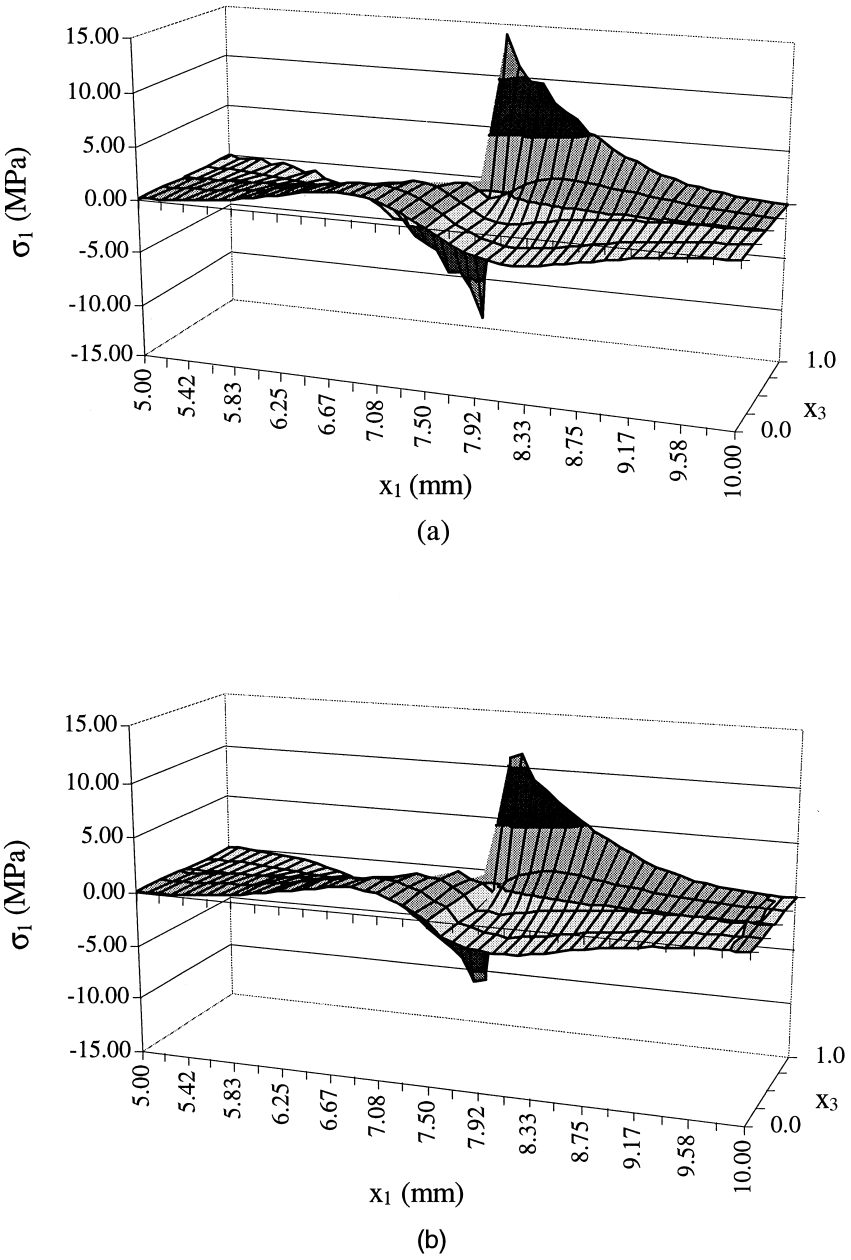

Fig. 3. Distribution of stress, σ_1, of the piezoceramic strip determined by (a) analytical model and (b) FEM approach.

4. Parametric study

The analytical model enables the effect of piezoceramic material characteristics on the stress and electric fields, and the extent of their coupling, to be studied. The governing equation in terms of

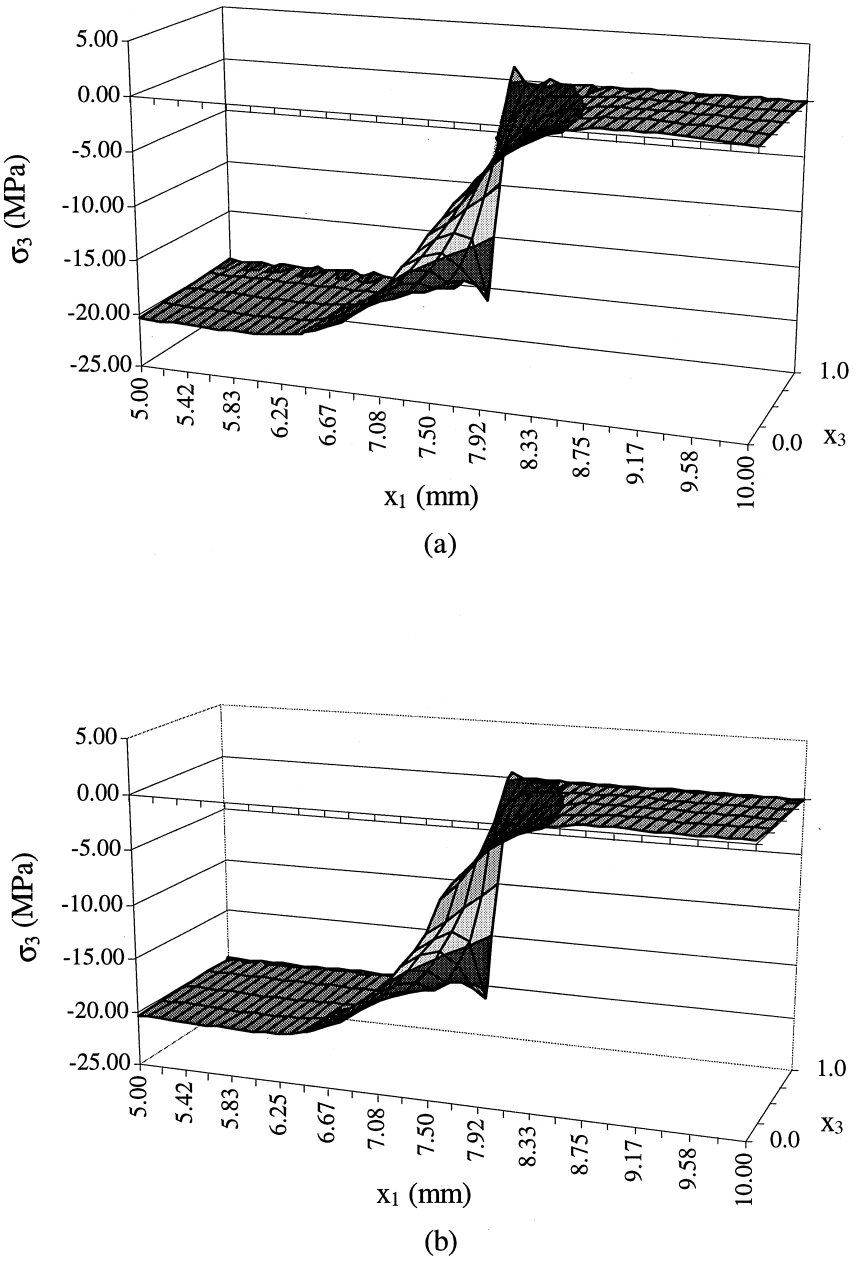

Fig. 4. Distribution of stress, σ_3, of the piezoceramic strip determined by (a) analytical model and (b) FEM approach.

the Airy stress function [eqn (19)] contains three non-dimensional material constants, β_1, β_2 and β_3. If $\beta_2 = \beta_3 = 0$, eqn (19) represents the problem in which the coupling between the stress and electric fields vanishes. Furthermore, when $\beta_1 = 2$, eqn (19) is reduced to the familiar biharmonic

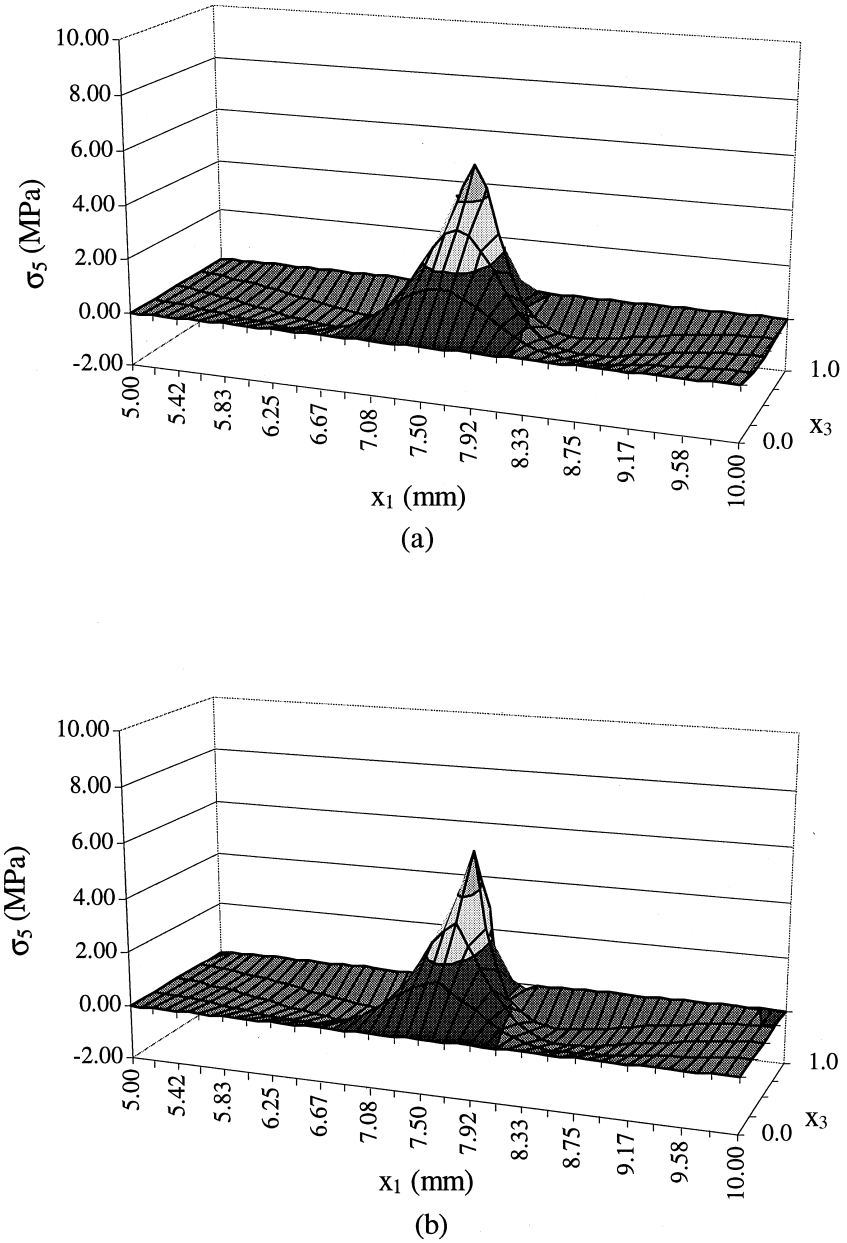

Fig. 5. Distribution of stress, σ_5, of the piezoceramic strip determined by (a) analytical model and (b) FEM approach.

equation for isotropic elastic materials. Therefore, there is a practical significance to study the effect of the non-dimensional parameters, β_1, β_2 and β_3, on the stress and the electric fields.

Table 1 lists data of elastic, piezoelectric and dielectric constants of some selected piezoceramic materials, and in Table 2 the corresponding values of non-dimensional constants, β_1, β_2 and β_3,

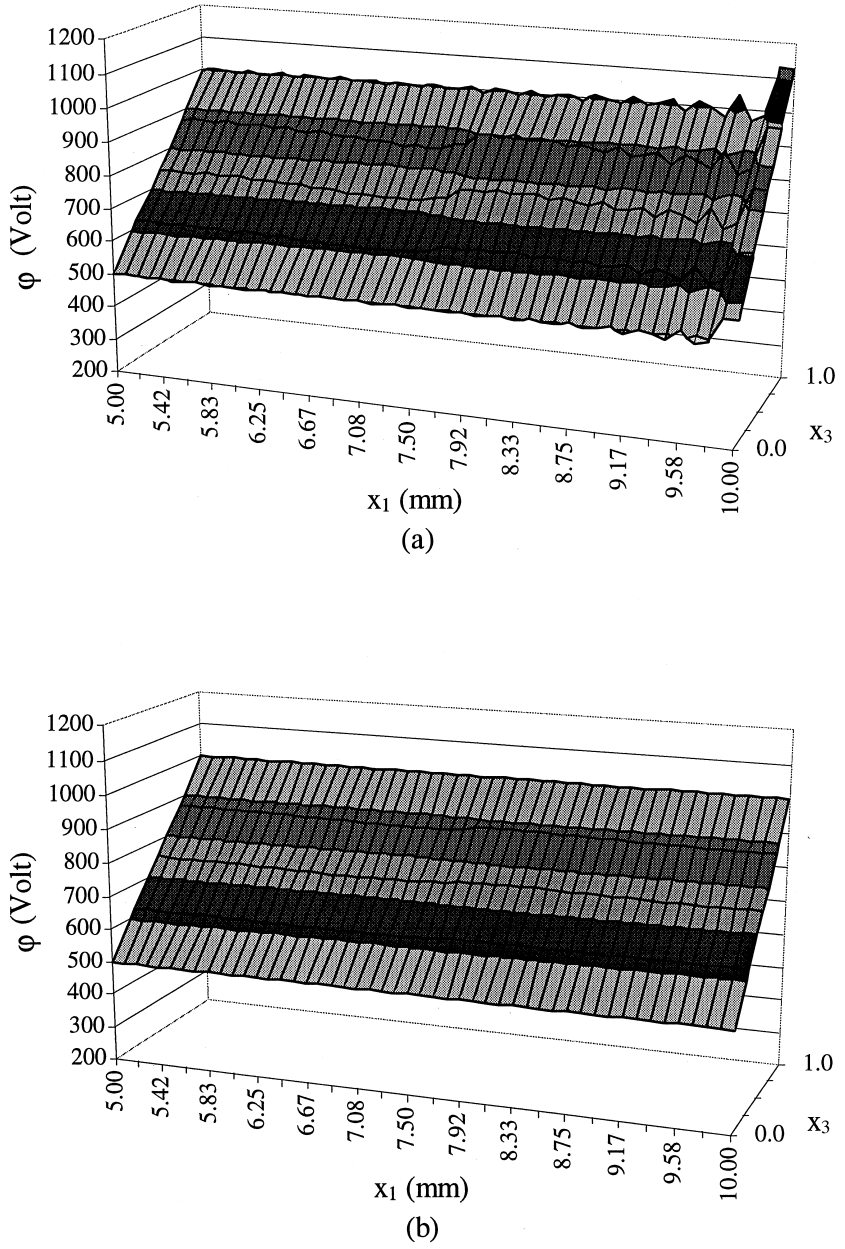

Fig. 6. Distribution of electric potential, φ, of the piezoceramic strip determined by (a) the analytical model and (b) FEM approach.

and dimensional constant, κ, are presented. The ranges of β_2 and β_3 for these piezoceramic materials are 0.0–0.35 and 0.0–0.187, respectively. In the following, a parametric study is performed on the variations of stresses and electric potential for $0 \leqslant \beta_2 \leqslant 0.6$, $\beta_1 = 1.44$, $\kappa = -16.61$ C/m^2 and $\beta_3 = 0.48 \cdot \beta_2$. The values of β_1, κ and β_3/β_2 are based upon PZT-5H.

Table 2
The parameters of some selected piezoceramics

	β_1	β_2	β_3	κ (C/m^2)
PZT-5H	1.439	0.350	0.169	−16.61
PZT-5	1.883	0.120	0.137	−10.49
PZT-4	1.985	0.128	0.187	−10.91
Ceramic-B	1.889	0.0485	0.0754	−6.74
VIBRIT 200	1.570	0.0632	0.0378	−7.21
VIBRIT 525	1.965	0.130	0.126	−12.10
Isotropic	2.0	0.0	0.0	

Variations of the non-dimensional stress components, σ_1/q_0 and σ_3/q_0, and electric potential, φ, with the non-dimensional coordinate variable, η, for several values of β_2, at three sections of the piezoceramic strip ($x_1 = 5$, $x_1 = 7$ and $x_1 = 9$ mm) are shown in Figs 7–9. It should be noted that the range of $0 \leqslant \beta_2 \leqslant 0.6$ and the corresponding values of β_3 ensure that $\gamma_1^2 - 4\gamma_2 < 0$ in eqn (25). Thus, the general solution of eqn (22) can be expressed by eqn (26). For the cases of $\gamma_1^2 - 4\gamma_2 = 0$ and $\gamma_1^2 - 4\gamma_2 > 0$, a slight change of the solution form of eqn (26) is expected.

The parameter β_2 influences the magnitude and distribution of the non-dimensional stress components and the electric potential. The profiles for stress components and electric potential become more uniform when β_2 decreases. Among the three sections, the maximum difference of the magnitude of stress components and electric potential occurs at the section of $x_1 = 7$ mm, near the edge of the distributed load. The magnitude of the non-dimensional stress component σ_1/q_0 is about 27% lower at $\beta_2 = 0.6$ than at $\beta_2 = 0$ for $\eta = 1$; σ_3/q_0 is about 4.8% lower at $\beta_2 = 0.6$ than at $\beta_2 = 0$ for $\eta = 1$; the electric potential φ is about 5% lower at $\beta_2 = 0.6$ than at $\beta_2 = 0$ for $\eta = 0.7$. Also, σ_1/q_0, is about 5% lower at $\beta_2 = 0.2$ than at $\beta_2 = 0$ for $\eta = 1$; σ_3/q_0 is about 2% lower at $\beta_2 = 0.2$ than at $\beta_2 = 0$ for $\eta = 1$; φ is about 2% lower at $\beta_2 = 0.6$ than at $\beta_2 = 0$ for $\eta = 0.7$.

5. Discussion and conclusions

(1) Comparison of the results obtained from the closed form solution with those from the FEM approach show that the present analytical approach is capable of analyzing 2-D piezoceramic problems.

(2) For the case that the voltage is added to the upper and lower edges of the strip, the assumption that $(\partial\varphi/\partial x_3) \gg (\partial\varphi/\partial x_1)$ is equivalent to the x_3-direction electric field, $\partial\varphi/\partial x_3$, induced by the stress field, is much smaller than that induced by the applied voltage. A comparison of the results from the FEM approach with those from the analytical model justifies this assumption.

(3) Based upon the assumption that the gradient of the electric potential in the x_1-direction is much smaller than that in the x_3-direction, the governing equations in terms of the Airy stress

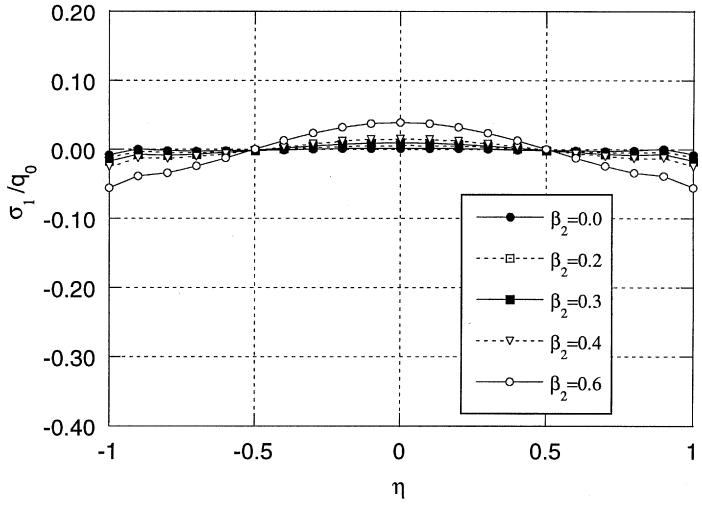

(a)

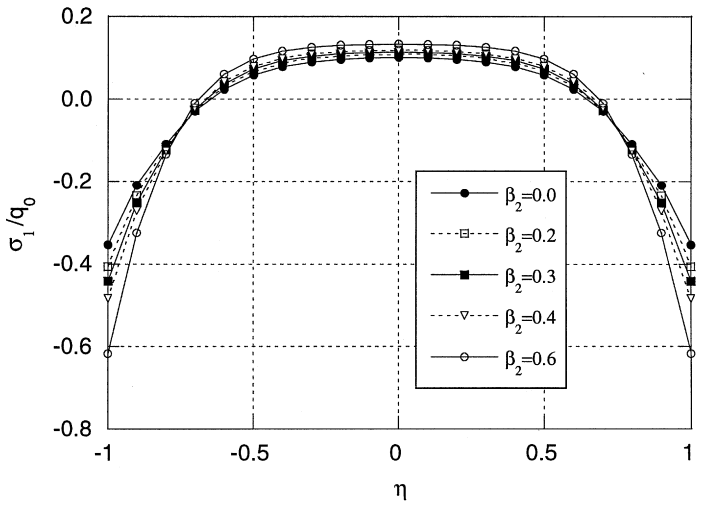

(b)

Fig. 7. Variation of non-dimensional stress component, σ_1/q_0, along η-axis for several values of the parameter β_2 at (a) $x_1 = 5.0$ mm, (b) $x_1 = 7.0$ mm, and (c) $x_1 = 9.0$ mm.

function and the electric potential function are uncoupled. Thus, the Airy stress function can be solved by using stress boundary conditions only, and the electric boundary condition does not influence the stress fields. The stress field is affected by the electric field through the piezoelectric and dielectric constants. However, for problems with displacement boundary conditions the electric boundary condition does influence the stress fields.

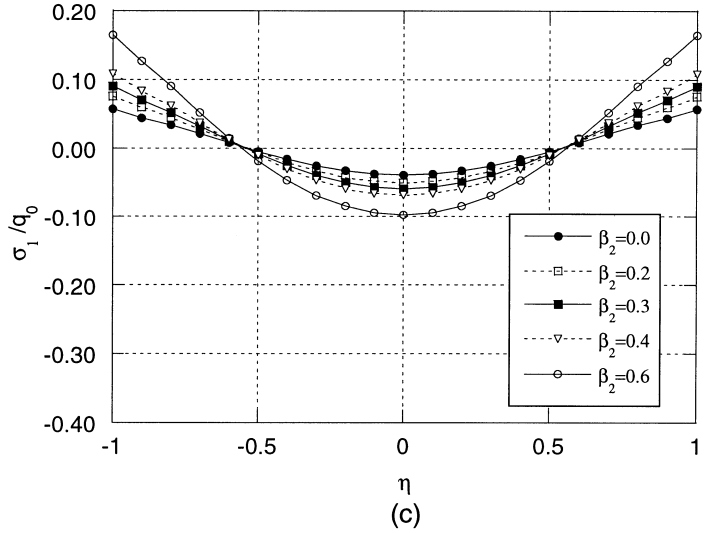

Fig. 7 (*continued*)

(4) By non-dimensionalization it can be seen from eqns (18)–(20) that the Airy stress function and the electric potential are affected by the material parameters, β_1, β_2, β_3 and κ, instead of the nine piezoceramic constants. An increase in d_{31} leads to higher β_2, β_3 and κ values, and consequently, a more pronounced effect of piezoelectricity on the stress fields.

(5) It can be seen from eqn (19) that β_1 consists of elastic compliance constants only, and β_2 and β_3 are expressed in terms of the elastic, piezoelectric and dielectric constants. Therefore, the parameters β_2 and β_3 signify the piezoelectric effect on the elastic field. For instance, $\beta_2 = \beta_3 = 0$ stands for the case of an elastic medium without any piezoelectric effect. Higher values of β_2 imply a more pronounced piezoelectric effect on the elastic field.

(6) Parametric study shows that among the three sections, the largest differences in the values of σ_1/q_0, σ_3/q_0 and φ for $\beta_2 = 0$ and $\beta_2 = 0.2$ occur at the section $x_1 = 7$ mm, and the differences are about 5, 2 and 2%, respectively. The values of β_2 of the piezoceramics selected in this study are less than 0.2 except for PZT-5H. Thus, for some piezoceramics, the effect of piezoelectricity on the elastic field is negligibly small.

(7) There is no significant influence of the parameter β_2 on the electric potential field. The electric potential is almost linear along the η-axis. An increase in β_2 causes a slight perturbation of the electric potential along the η-axis. Among the three sections considered, the biggest perturbation occurs at the section of $x_1 = 7.0$ mm.

(8) Identification of the parameter, β_1, β_2 and β_3, greatly facilitates the study of coupling effects in piezoelectric ceramics.

Acknowledgements

This work was supported by the Office of Naval Research through the MURI program at Rutgers, The State University of New Jersey.

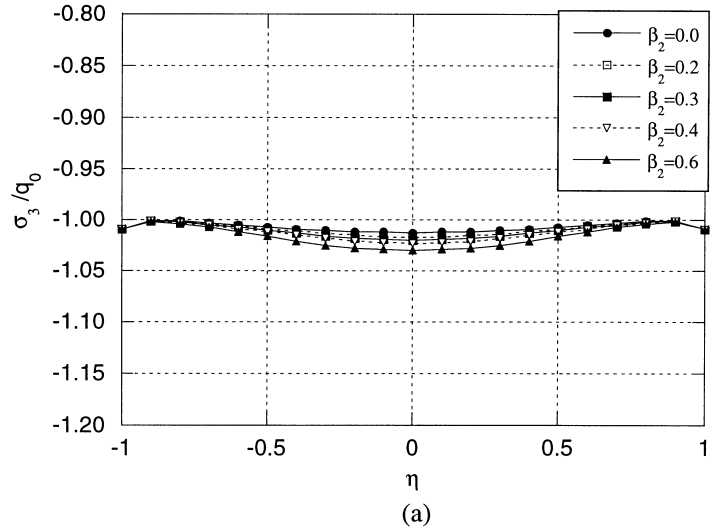

(a)

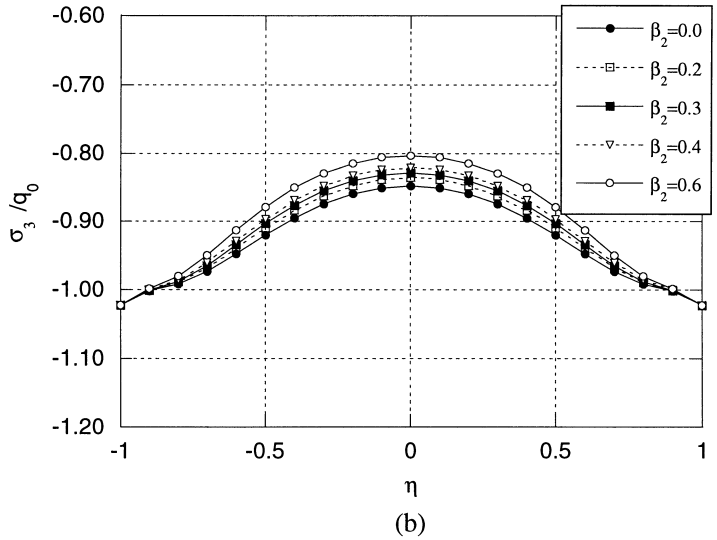

(b)

Fig. 8. Variation of non-dimensional stress component, σ_3/q_0, along η-axis for several values of the parameter β_2, at (a) $x_1 = 5.0$ mm, (b) $x_1 = 7.0$ mm, and (c) $x_1 = 9.0$ mm.

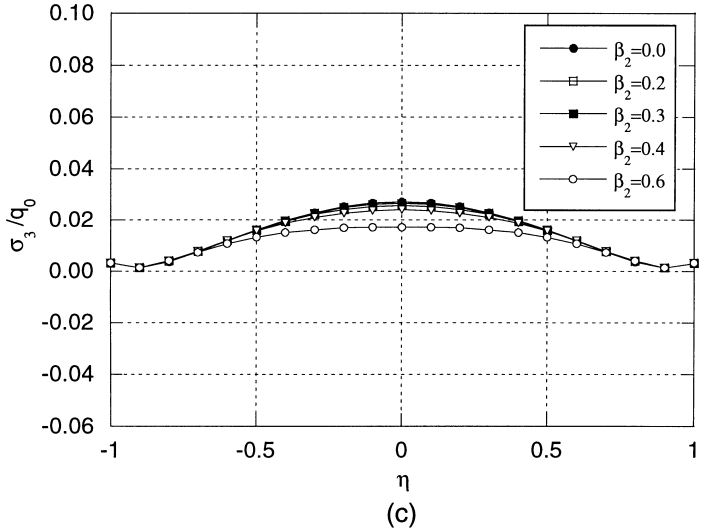

Fig. 8 (*continued*)

Appendix

$$F_n(\eta) = (e^{p_n\eta} + e^{-p_n\eta})C_{n1}\cos q_n\eta + (e^{p_n\eta} - e^{-p_n\eta})C_{n2}\sin q_n\eta \tag{A1}$$

$$\begin{aligned} F_n'(\eta) &= p_n(e^{p_n\eta} - e^{-p_n\eta})C_{n1}\cos q_n\eta - q_n(e^{p_n\eta} + e^{-p_n\eta})C_{n1}\sin q_n\eta \\ &\quad + p_n(e^{p_n\eta} + e^{-p_n\eta})C_{n2}\sin q_n\eta + q_n(e^{p_n\eta} - e^{-p_n\eta})C_{n2}\sin q_n\eta \end{aligned} \tag{A2}$$

$$\begin{aligned} F_n''(\eta) &= p_n^2(e^{p_n\eta} + e^{-p_n\eta})C_{n1}\cos q_n\eta - 2p_nq_n(e^{p_n\eta} - e^{-p_n\eta})C_{n1}\sin q_n\eta \\ &\quad - q_n^2(e^{p_n\eta} + e^{-p_n\eta})C_{n1}\cos q_n\eta + p_n^2(e^{p_n\eta} - e^{-p_n\eta})C_{n2}\sin q_n\eta \\ &\quad + 2p_nq_n(e^{p_n\eta} + e^{-p_n\eta})C_{n2}\cos q_n\eta - q_n^2(e^{p_n\eta} - e^{-p_n\eta})C_{n2}\sin q_n\eta \end{aligned} \tag{A3}$$

$$\begin{aligned} I_n(\eta) &= \frac{C_{n1}}{p_n^2 + q_n^2}(p_n\cos q_n\eta + q_n\sin q_n\eta)e^{p_n\eta} \\ &\quad + \frac{C_{n1}}{p_n^2 + q_n^2}(-p_n\cos q_n\eta + q_n\sin q_n\eta)e^{-p_n\eta} \\ &\quad + \frac{C_{n2}}{p_n^2 + q_n^2}(-q_n\cos q_n\eta + p_n\sin q_n\eta)e^{p_n\eta} \\ &\quad + \frac{C_{n2}}{p_n^2 + q_n^2}(q_n\cos q_n\eta + p_n\sin q_n\eta)e^{-p_n\eta} \end{aligned} \tag{A4}$$

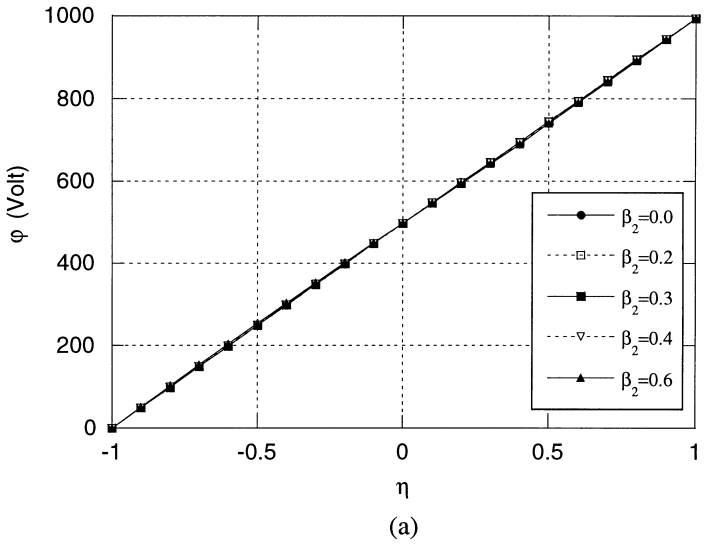

(a)

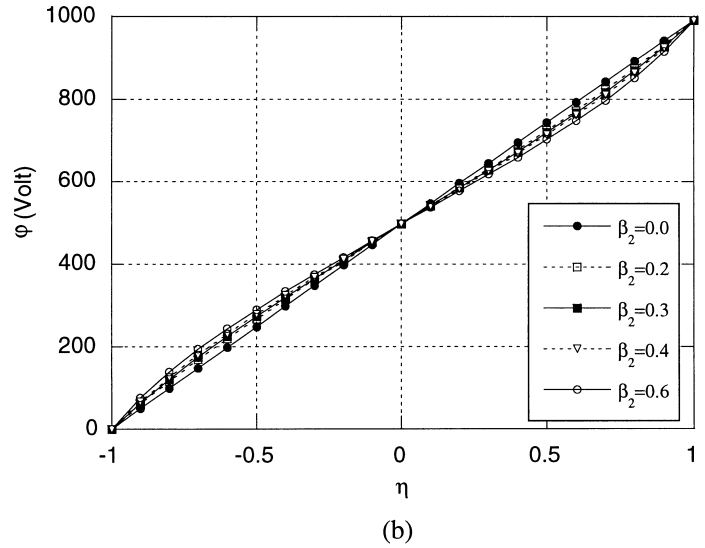

(b)

Fig. 9. Variation of electric potential, φ, along η-axis for several values of the parameter, β_2, at (a) $x_1 = 5.0$ mm, (b) $x_1 = 7.0$ mm, and (c) $x_1 = 9.0$ mm.

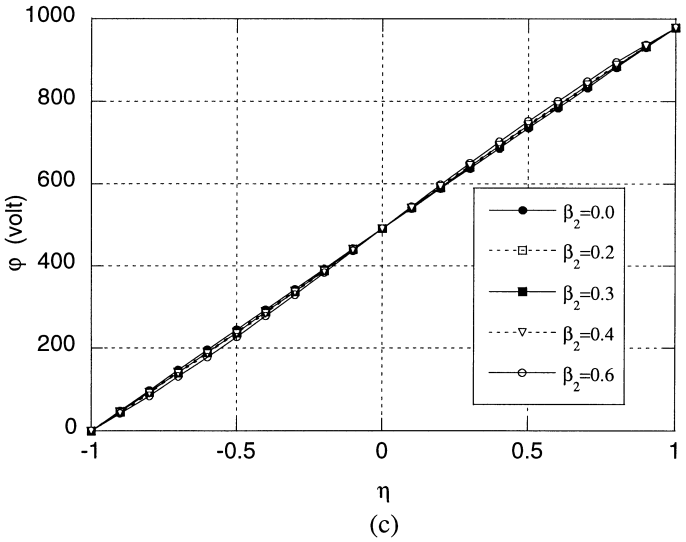

(c)

Fig. 9 (*continued*)

$$C_{n1} = \frac{a_{22}}{a_{11}a_{22} - a_{12}a_{21}} \frac{b_n}{\rho_n}$$

$$C_{n2} = -\frac{a_{21}}{a_{11}a_{22} - a_{12}a_{21}} \frac{b_n}{\rho_n} \tag{A5}$$

where

$$a_{11} = (e^{p_n} + e^{-p_n}) \cos q_n, \quad a_{12} = (e^{p_n} - e^{-p_n}) \sin q_n$$

$$a_{21} = p_n(e^{p_n} - e^{-p_n}) \cos q_n - q_n(e^{p_n} + e^{-p_n}) \sin q_n$$

$$a_{22} = p_n(e^{p_n} + e^{-p_n}) \sin q_n - q_n(e^{p_n} - e^{-p_n}) \cos q_n$$

$$D_{n1} = \frac{1}{2}(d_n - e_n) - \alpha_n^2 \frac{\beta_3}{\kappa H} I_n(1)$$

$$D_{n2} = \tfrac{1}{2}(d_n + e_n). \tag{A6}$$

References

Data Sheet, 1990. Piezoceramics. Vernitron Piezoelectric Division, Bedford, Ohio.

Dogan, A., Newnham, R.E., 1994. Flextensional Cymbal Transducer. USA Patent application, PSU Invention Disclosure No. 94-1375.

Greenberg, M.D., 1988. Advanced Engineering Mathematics. Prentice-Hall, New Jersey, 451–470.

Kagawa, Y., Tsuchiya, T., Kataoka, T., 1996. Finite element simulation of dynamic responses of piezoelectric actuators. Journal of Sound and Vibration 191(4), 519–538.

Newnham, R. E., 1997. Molecular mechanisms in smart materials. MRS Bulletin, pp. 20–34.

Newnham, R.E., Xu, Q.C., Yoshikawa, 1992. Transformed Stress Direction-Acoustic Transducer. U.S. Patent 4,999,819.

Park, S.B., Sun, C.T., 1995. Effect of electric field on fracture of piezoelectric ceramics. International Journal of Fracture 70, 203–216.

Rogacheva, N. N., 1994. The Theory of Piezoelectric Shells and Plates. CPR Press, Inc., Boca Paton, Florida.

Tiersten, H. F., 1969. Linear Piezoelectric Plate Vibrations. Plenum Press, New York.

Tzou, H.S., Tseng, C. I. 1990. Distributed piezoelectric sensor/actuator design for dynamic measurement/control of distributed parameter systems : a piezoelectric finite element approach. Journal of Sound and Vibration 138(1), 17–34.

Visual Numerics, Inc., 1994. IMSL Math/Library. Houston, Texas.

Zelenka, J., 1986. Piezoelectric Resonators and their Application. Elsevier, Amsterdam, Netherlands.

Zhang, Q. M., Cheng, J., Wang, H., Zhan, J., Cross, L. E., Trottier, M. C., 1995. A new transverse piezoelectric mode 2-2 piezocomposite for underwater transducer applications. IEEE Trans. Ultrason. Ferroelect. Frequ. Cont. 42(4), 774–780.